Light-Induced Equilibration Kinetics in Membrane-Bound Photosynthetic Reaction Centers: Nonlinear Dynamic Effects in Multiple Scattering Media

Alexander O. Goushcha,[*,†,§] **Anthony J. Manzo,**[†] **Valery N. Kharkyanen,**[‡]
Rienk van Grondelle,[||] **and Gary W. Scott**[*,†]

Department of Chemistry, UC Riverside, Riverside, California 92521,
Institute of Physics, National Academy of Science, Ukraine, Kyiv, Ukraine, Semicoa,
Costa Mesa, California 92626, and Faculty of Physics and Astronomy, Vrije Universiteit,
Amsterdam, The Netherlands

Received: August 12, 2003; In Final Form: December 22, 2003

Nonequilibrium dynamic effects in membrane-bound reaction centers (RCs) from photosynthetic bacteria are studied for the first time. We show that the accumulation of slow conformational changes triggered by charge-separation events in the RCs control system dynamics and depend on illumination conditions in a way similar to that for isolated RCs. The light-induced, transient kinetics of membrane-bound RCs are described using a model of electron-conformational transitions governed by system diffusion along the surface of a double-well, effective adiabatic potential. The light-triggered conformational transitions in the chromatophores are estimated to occur at an actinic light intensity at least 10 times lower than that needed for conformational transitions in isolated RCs. This finding is attributed to efficient, multiple-scattering effects that occur in sample with membranes. Related optical properties of the chromatophores as a disordered system with multiple light scattering are characterized for the first time.

Introduction

Recent studies of equilibration kinetics following a train of actinic flashes applied to light-adapted, isolated, photosynthetic reaction centers (RCs) showed that these kinetics are affected by the method of sample preparation.[1−3] In particular, a pronounced, slow relaxation phase following flash excitation is prominent in the equilibration kinetics of RCs isolated from the purple bacteria *Rhodobacter (Rb.) sphaeroides* after dialysis against an excess of two different detergents, either Triton X-100 (0.05%, pH 7.5) or sodium (Na) cholate (0.1%, pH 8.0). The slow relaxation phase was not as pronounced in RCs prepared with the detergent lauryl-*N*,*N*,-dimethylamine-*N*-oxide (LDAO, 0.05% LDAO, pH 7.5). The difference in equilibration kinetics was attributed to variations in the dynamic properties of RCs that were prepared using different detergents. The structural diffusion constant of the charge neutral state was determined to be among the main parameters responsible for the emergence of a slow relaxation component in the kinetics of isolated RCs.[1,2]

Despite the obvious interest in a comparison of results from studies of nonequilibrium dynamic effects in isolated RCs with those in chromatophores, the latter studies have not previously been performed because of apparent difficulties in deducing an unambiguous interpretation of the results of light-induced effects on photosynthetic membranes. The interpretation of experimental results on the dynamics of membrane-bound RCs is confounded by significant overlap of RC absorption with that of antennae complexes in these systems. Further, the presence of the water-soluble protein cytochrome c2 and the membrane bound cytochrome bc1 complex complicate the interpretation of experimental results on charge-transfer kinetics in such chromatophores.[4−7]

Studies of RC dynamics in photosynthetic membranes and the interpretation of these dynamics in terms of light-induced electron-transfer (ET) events is considerably simplified for antennae-free mutants of *Rb. sphaeroides* RCs, e.g., the RC01 strain described in ref 8. Although cytochrome c2 can be relatively easily removed from a chromatophore suspension, the cytochrome bc1 complex is tightly bound to the membrane. This complex could participate in oxidation−reduction reactions with membrane-bound RCs, again complicating the kinetics and their interpretation. When in a close proximity to the bacteriochlorophyll dimer *P* of RC, cytochrome c1 of the cytochrome bc1 complex may donate an electron to the (photo)oxidized dimer P^+. This event may be initiated by oxidation−reduction reactions between cytochrome c1 and either the high-potential heme (close to the Q_i site of cytochrome bc1) or the low-potential heme (close to the Q_o site of cytochrome b molecule, both of which are a part of a cytochrome bc1 complex.[4,6,9] However, rereduction of P^+ by a cytochrome bc1 complex under continuous illumination conditions can be blocked by cytochrome bc1 inhibitors such as myxothiazol (which specifically inhibits the Q_o site) or antimycin (which inhibits the Q_i site).[6,7,9−11] Use of these inhibitors provides a method to experimentally isolate the kinetics of forward and back ET reactions and their dependence on light adaptation in membrane-bound RCs.

The present work addresses another interesting feature of a chromatophore suspension. Such samples of photosynthetic membranes may be considered as highly disordered systems with a highly efficient excitation mechanism via multiple light

* Authors to whom correspondence should be addressed. E-mail: GaryScott@citrus.ucr.edu (G.W.S.); ogoushcha@semicoa.com, goushcha@ucrac1.ucr.edu (A.O.G.). Fax: (909) 787-2243 (G.W.S.); (714) 557-4541 (A.O.G.).
† University of California−Riverside.
‡ National Academy of Science.
§ Semicoa.
|| Vrije Universiteit.

scattering upon illumination. For other systems of this type, nonlinear optical effects such as enhanced absorption and backscattering,[12,13] a dramatic decrease in the lasing threshold,[14] and an Anderson-type light localization[15] all have been observed. The current paper presents our initial results of studies into nonequilibrium dynamic effects in a highly scattering medium on membrane-bound, photosynthetic RCs. We show experimental results of light-induced RC absorbance changes that can be understood in the context of enhanced absorption due to multiple light scattering.

Material and Methods

Samples. Membrane-bound RCs lacking both LH1 and LH2 antenna complexes (strain RCO1) were generously provided by Dr. Michael R. Jones. This strain, characterized in ref 8, is photosynthetically competent and contains active cytochrome bc1 complexes (the ratio of reaction centers to bc1 complexes was approximately 3:1 in these membranes). The samples were depleted of cytochrome c2. Concentrated membranes were mixed with a buffer solution of Tris−HCl (20 mM tris-hydroxymethylamine methane) with a pH of 8.0. The RC concentrations in membranes were determined from absorption spectra using a molar absorption coefficient of 2.88×10^5 M^{-1} cm^{-1} at 802 nm.[16]

The membrane solution was filtered using 0.45-μm cartridge-type filters, and the RC concentration was estimated as ca. 0.7 $\times 10^{-6}$ M. The cytochrome bc1 inhibitors myxothiazol (Sigma) and antimycin (Sigma) were each dissolved in a small amount of ethanol. The myxothiazol solution was added first to a portion of membrane solution in a 5-fold excess. Antimycin and myxothiazol were each added at 5 times the concentration of RCs in a second sample. The three samples, one with pure membranes, the second one containing membranes with myxothiazol, and the third one containing membranes with both myxothiazol and antimycin, were left overnight at 4 °C for subsequent use in experiments at room temperature.

Isolated RCs were prepared from photosynthetic membranes using the detergent LDAO according to the procedure described previously.[17] Following purification on a column of oxiapatite, RCs were suspended in 10 mM Tris−HCl buffer with 0.05% LDAO, pH 7.5. The RC suspension was then dialyzed against an excess of the detergent Triton X-100 (0.05%, pH 7.5) according to conventional methods. See ref 18 for more details about RC isolation and sample preparation. The occupancy of the Q_B site after the isolation procedure was 30−40% as measured by the slow phase amplitude in the charge recombination kinetics following a saturating flash. No quinone reconstitution procedure was used. The samples were checked for the absence of cytochrome c2. The absorbance ratio A_{280}/A_{800} that characterizes the sample purity was in the range 1.25−1.35.

Experimental Setup. Transient absorption experiments were carried out on samples of membrane-bound photosynthetic RCs using the optical setup described below. Samples in a 1-cm quartz cuvette were placed in the sample compartment. A quartz tungsten−halogen lamp coupled to a monochromator was used for the source of measuring (monitoring) light at 865 nm (bandwidth = 20 nm). The monitoring light was also filtered with a red cutoff filter RG-630 (Schott) and different neutral density filters for intensity control. An iris diaphragm was placed in the monitoring beam path to control the beam diameter. The monitoring light intensity was ≤5 μW/cm^2. After passing through the sample, the light was focused on to the entrance slit of the second monochromator also set at $\lambda = 865$ nm to eliminate ambient and scattered actinic light.

As a source of excitation light, we used either a continuous-wave (cw) white light from a tungsten−halogen lamp or pulses from a dye laser. cw actinic light was filtered with a 10-cm path water filter and cutoff filter OG-550 (Schott). An electronic shutter was placed in the cw beam path to switch the light on and off. A set of neutral density filters was also used to control the light intensity on the sample in a range up to $I_0 = 4.5$ mW/cm^2. Special care was used to ensure uniform photoexcitation of the sample path perpendicular to the monitoring beam. A pinhole diaphragm was placed in this path to provide excitation of a particular part of the total volume of a sample as appropriate. A Quanta-Ray DCR-3 Pulsed Nd−YAG Laser (Spectra-Physics) in conjunction with a Quanta-Ray PDL-2 dye laser served as the source of the actinic light pulses. The dye laser was tuned to 605 nm using Rhodamine 640 as the dye. The pulse energy at 605 nm was ∼50 mJ, and care was taken to provide a uniform excitation of the membranes across the surface of the sample (ca. 1 cm^2 excitation area). Both the cw and pulsed excitation of the sample were at a 90° angle to the monitoring beam.

The intensities of the monitoring light, cw actinic light, and pulsed laser excitation were monitored simultaneously with photodiodes coupled to wide bandwidth preamplifiers to account for any instability in the light sources. The signals from the preamplifiers were acquired with a plug-in data-acquisition board (Keithley DAS-1801 ST-DA). This board triggered the shutter and the laser pulse.

Lock-in amplifier techniques were used in specific experiments to reduce noise during data acquisition at slow rates and/or over long time intervals. In these experiments, an electro-mechanical chopper was inserted into the monitoring light beam. The frequency of the chopper was adjusted to about 1290 Hz.

Modeling. The calculation of RC absorption changes with variation of actinic light intensity is based on the model previously described for a reduced two-level scheme of RC redox states[1,2,19,20]

$$\frac{\partial P_P(t,x)}{\partial t} = L_P P_P(t,x) - I P_P(t,x) + k_{AP} e^{-x} P_B(t,x)$$

$$\frac{\partial P_B(t,x)}{\partial t} = L_B P_B(t,x) + I P_P(t,x) - k_{AP} e^{-x} P_B(t,x) \quad (1)$$

$$L_i = D_i \frac{\partial}{\partial x}\left(\frac{dV_i(x)}{dx} + \frac{\partial}{\partial x}\right) \quad x = \frac{\Delta G_{AB}}{k_B T} \quad i = P,B$$

in which $P_P(t,x)$ and $P_B(t,x)$ describe the time evolution of the RC distribution function over a single dimensionless structural variable x for two different redox states, PQ_AQ_B (neutral state) and $P^+Q_AQ_B^-$ (charge separated state), respectively. I is the photoexcitation intensity, in units of single RC photoexcitations, and k_{AP} is the rate of electron recombination from the primary quinone acceptor Q_A to the bacteriochlorophyll dimer P. In eq 1 D_i is the diffusion constant, ΔG_{AB} is the difference of the quasi-free energies for electron localization on Q_A and on Q_B, k_B is the Boltzmann constant, T is an absolute temperature, V_P and V_B are the redox potentials in units of $k_B T$[1,2]

$$V_i(x) = \frac{1}{2} k_i (x - x_i)^{2(1+\alpha_i)} \frac{\gamma_i}{\gamma_i^2 + (x - x_i)^2} \quad (2)$$

in which γ_i and $\alpha_i < 1$ are the anharmonicity parameters, and x_P and x_B are the minimum positions for the charge neutral

Nonequilibrium Dynamics in Reaction Centers

J. Phys. Chem. B, Vol. 108, No. 8, 2004 **2719**

(index P) and charge separated (index B) states of RC, respectively.

The rate of electron recombination from the secondary quinone acceptor Q_B is written in eq 1 as $k_r(x) = k_{AP} e^{-x}$. Such a dependence for RCs has been discussed in details previously[1,2,19,20,22] and was based on the fact that the rate constant of electron transfer from Q_B to P at normal physiological conditions is given by

$$k_{Q_B \to P} = k_{Q_A \to P} \frac{k_{Q_B \to Q_A}}{k_{Q_A \to Q_B}} = k_{Q_A \to P} \exp\left(-\frac{\Delta G_{AB}}{k_B T}\right)$$

By assumption that

$$k_r(x) = k_{Q_A \to P} \quad \text{and} \quad x = \frac{\Delta G_{AB}}{k_B T}$$

we obtain the assumed expression for $k_r(x)$. In the above consideration, we took into account that the slow component of structural rearrangements, triggered by electron localization on Q_B causes slow changes in the ΔG_{AB} value due to interaction with the polar surroundings of the secondary electron acceptor in RCs. The relationship $k_r(x) = k_{AP} e^{-x}$ is quite reasonable, irrespective of specific nature of x and causes no restriction of generality. Such an approach allows us to model in a quite straightforward and simple way the light-intensity-controlled dynamics of electron transfer in photosynthetic reaction center.

Slow structural changes are described as diffusion along the surface of a light-intensity-controlled, nonequilibrium adiabatic potential $V_I^{eff}(x)$.[19,20] This potential is described by the equation

$$\frac{dV_I^{eff}(x)}{dx} = \frac{dV_P(x)}{dx} \rho_P^{st}(x;I) + \frac{dV_B(x)}{dx} \rho_B^{st}(x;I) \quad (3)$$

in which

$$\rho_P^{st}(x;I) = \frac{k_{AP} e^{-x}}{I + k_{AP} e^{-x}} \quad \rho_A^{st}(x;I) = \frac{I}{I + k_{AP} e^{-x}}$$

are the stationary-state populations of the electronic states at a fixed value of the structural variable x and for a given photoexcitation intensity I. The equation of motion for the structural variable x in the adiabatic approximation can be written as follows

$$\frac{\partial P(t;x)}{\partial t} = D \frac{\partial}{\partial x}\left[\frac{1}{k_B T} \frac{\partial V_I^{eff}(x)}{\partial x} P(t;x) + \frac{\partial P(t;x)}{\partial x}\right] \quad (4)$$

in which $P(t;x) = \Sigma_i P_i(t;x)$ is the distribution function density of the structural variable. The stationary state solution of eq 4 becomes

$$P(\infty;x) = \frac{e^{-V_I^{eff}(x)/k_B T}}{z(I)}$$

in which

$$z(I) = \int dx \, e^{-V_I^{eff}(x)/k_B T}$$

See refs 1, 2, and 20 for details about the generalized adiabatic potential and the slow, control structural variable (mode) for the RC.
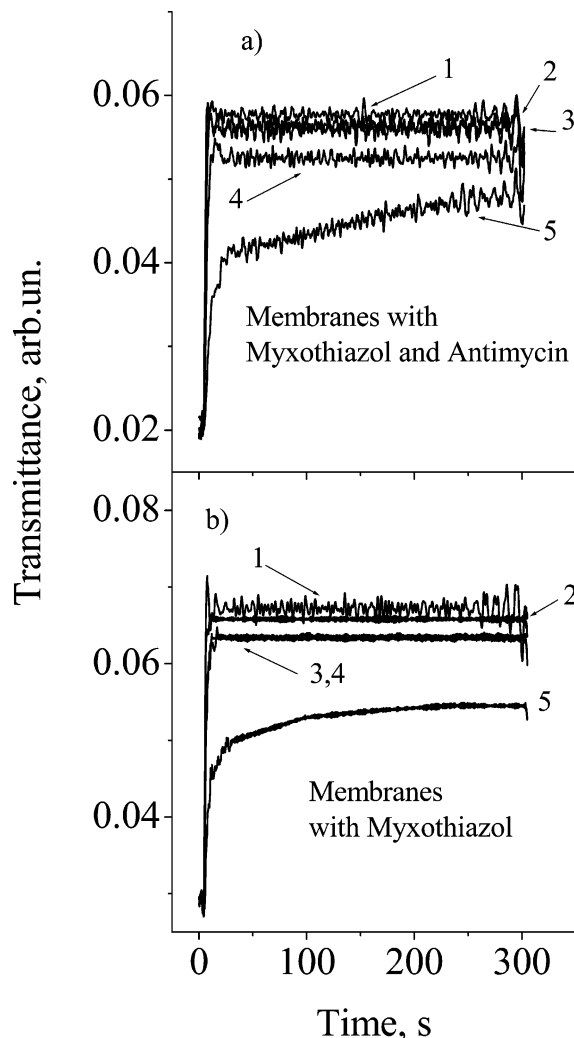

Figure 1. Bleaching kinetics for two different samples of membrane-bound RCs at various photoexcitation intensities: (1) I_0; (2) $0.5I_0$; (3) $0.2I_0$; (4) $0.1I_0$; and (5) $0.02I_0$. I_0 represents a light flux of ca. 4.5 mW/cm^2 ($\lambda \approx 600-900$ nm).

Equations 1−4 were used to model experimental results on equilibration kinetics of membrane-bound RCs.

Results

Multiple Scattering Effects in Excitation Dynamics of Membrane-Bound RCs. Figure 1 shows dependence of membrane-bleaching kinetics at the bacteriochlorophyll dimer absorption band (865 nm) at different photoexcitation intensities. Both the sample with myxothiazol (graph b in Figure 1) and the sample with myxothiazol and antimycin (graph a in Figure 1) show a bleaching saturation of less than 10 s after initiation of cw actinic light for excitation intensities $I_{ex} \geq 0.1\,I_0$, in which I_0 is a cw excitation intensity of ca. 4.5 mW/cm^2. The RC bleaching amplitude is nearly independent of the cw actinic light intensity for $I_{ex} \geq 0.1\,I_0$. See curves 1−4 on both graphs of Figure 1. At lower actinic light intensities, $I_{ex} < 0.1\,I_0$, the bleaching amplitude is smaller, and the equilibration kinetics reveal a slow phase with a characteristic time constant of >50 s (curve 5 in parts a and b of Figure 1). These observations are quite different from what one obtains for isolated RCs under similar illumination conditions.[1,21]

In analogous experiments with isolated RCs, the bleaching amplitude at 865 nm showed a pronounced dependence on the actinic light intensity over the entire photoexcitation intensity
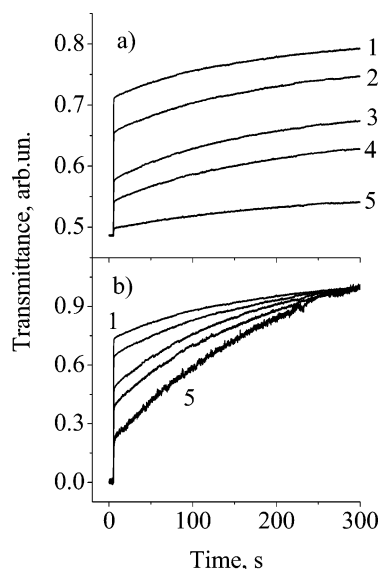
Figure 2. Bleaching kinetics of isolated RCs at various photoexcitation intensities. (a) Measured bleaching kinetics at the same excitation intensities shown in Figure 1 for membrane-bound RCs: (1) I_0; (2) $0.5I_0$; (3) $0.2I_0$; (4) $0.1I_0$; and (5) $0.02I_0$. (b) The same results as presented in graph a but normalized and superimposed.

range. See Figure 2a. The equilibration kinetics for each I_{ex} was biphasic, and the largest amplitude for the slow relaxation phase was measured at the lowest value of the actinic light intensity. The normalized transmittance curves for isolated RCs are presented in Figure 2b. Note that these RC equilibration kinetics are described within a formalism of nonequilibrium dynamics with a slow structural diffusion along the surface of an adiabatic potential.[1,2]

Under the reasonable assumption of an equal-absorption oscillator strength at 865 nm for both isolated and membrane bound RCs, the difference in bleaching kinetics of the two systems can be explained by assuming that the excitation rate for each macromolecule, at the same incident actinic light intensity, is higher for membrane-bound RCs than for isolated RCs. To check this assumption, we studied the dependence of absorption bleaching kinetics with an excitation beam cross section at a fixed photoexcitation intensity I_{ex}. Specifically, the cw actinic light intensity was kept constant, but a pinhole diaphragm was placed at the photoexcitation surface of the cuvette thereby limiting the photoexcitation beam diameter. The monitoring beam diameter was set at ~3 mm. The results of these studies are presented in Figure 3.

Curves 1, 2, and 3 in each graph of Figure 3 correspond to an excitation beam cross section of 10×10 mm^2, 5-mm diameter, and 3-mm diameter, respectively. In the case of membrane-bound RCs, a decrease in the excitation beam cross section causes only a slight decrease in the bleaching amplitude. See graphs a and b in Figure 3. In contrast, the bleaching amplitude for isolated RCs drops by almost a factor of 3 times when the actinic light beam cross section is decreased from 10×10 mm^2 to 5 mm in diameter (see curves 1 and 2 in Figure 3c) and decreases by almost another factor of 3 upon reducing the beam diameter down to 3 mm. See curve 3 in Figure 3c.

In contrast to the bleaching amplitudes, the bleaching kinetics were nearly independent of the actinic beam cross section for the case of isolated RCs (see Figure 4c), whereas they showed a strong dependence on the photoexcitation beam cross section for the case of membrane-bound RCs. See parts a and b of Figure 4. For membrane-bound RCs, no slow relaxation phase was observed with the full (10×10 mm^2) excitation beam. In

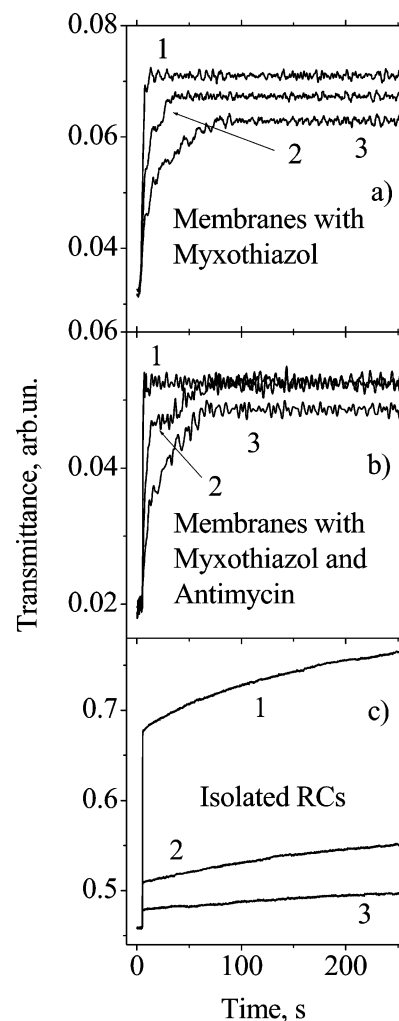**Figure 3.** Dependence of RC bleaching kinetics on the excitation beam cross section for three different samples: (1) full beam (10×10 mm^2); (2) 5-mm diameter beam; and (3) 3-mm diameter beam.

this case, however, decreasing the excitation beam cross section produced a slow relaxation phase with an amplitude increasing upon further decrease of the actinic beam cross section. In contrast, for isolated RCs, the slow phase in the absorption bleaching kinetics was always observed, and its amplitude was almost independent of the excitation beam cross section. Compare curves 1, 2, and 3 in graphs a and b of Figure 4 with the corresponding curves in the graph c of Figure 4.

Ideally, for isolated RCs, one would expect to obtain identical normalized curves for the bleaching kinetics measured at various cross sections of the actinic beam. However, diffusion of the molecules in to and out of the excitation volume might modify the observed kinetics. This effect is not important if all molecules in the sample are excited, but it can become significant if the excitation cross section is significantly smaller than the cross section of the sample. In this latter case, the diffusion of molecules in to and out of the excitation volume may result in an apparent decrease of the photoexcitation intensity. This could be the reason for the differences in curves 2 and 3 from curve 1 in Figure 4c. The effect of molecular diffusion in to and out of the excitation volume is less significant for heavier, larger molecules with smaller diffusion coefficients. Thus, such an effect should not strongly affect results obtained for membrane-bound RCs.

Obviously, molecular diffusion and multiscattering effects play against one another, and one might attempt to explain
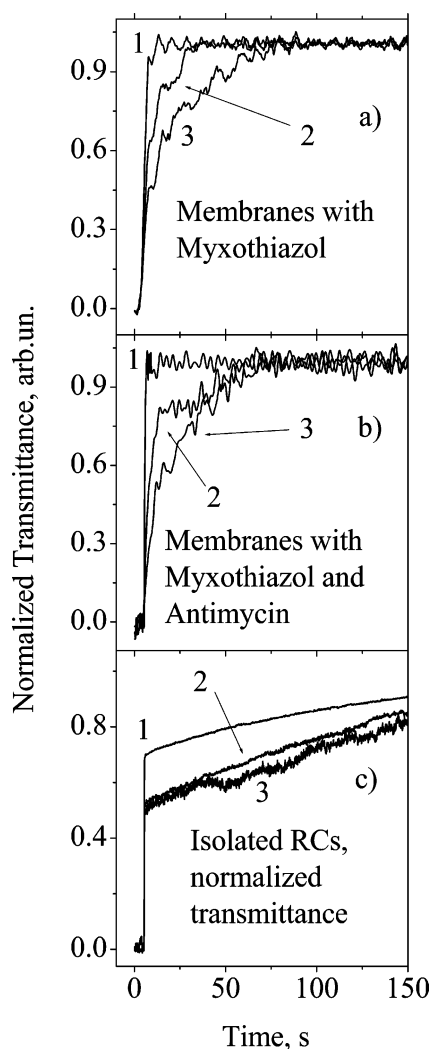
Nonequilibrium Dynamics in Reaction Centers

J. Phys. Chem. B, Vol. 108, No. 8, 2004 **2721**

Figure 4. Normalized bleaching kinetics for the samples and beam cross sections shown in Figure 3: (1) full beam (10 × 10 mm²); (2) 5-mm diameter beam; and (3) 3-mm diameter beam.

differences in relaxation kinetics for the membrane bound RCs at different excitation beam cross sections by the molecular diffusion effects. However, such an explanation can be ruled out by the following considerations. For isolated RCs, there is no difference in relaxation kinetics measured at 3 and 5 mm excitation beam diameter (curves 2 and 3 in Figure 4c). It means that molecular diffusion effects, if important, are equally pronounced for the case of each beam diameter. One might expect a similar behavior at the same excitation beam cross sections in the case of membranes. However, the relaxation kinetics for the 3-mm diameter excitation beam is considerably slower than for the 5-mm diameter beam (compare curves 3 and 2 in parts a and b of Figure 4), which favors an explanation other than molecular diffusion for the delay in kinetics. Taking into account the results for different excitation light intensities (see Figures 1 and 2 and discussion above), we can attribute changes in relaxation kinetics with excitation beam cross section in membranes as mainly due to multiscattering effects. We do not consider in the present work effects of molecular diffusion assuming that these effects are the second-order importance effects for the membrane-bound RCs.

Comparison of the Effective Excitation Intensity of Membrane-Bound RCs with that of Isolated RCs. Results such as those illustrated in Figures 1 and 2 can be used to determine the relative effective excitation intensities for samples

of isolated and membrane-bound RCs. We showed previously that the stationary-state bleaching amplitude of a RC sample should obey a Langmuir saturation law if slow, light-induced conformational changes in the RCs do not occur and/or the survival time of the charge-separated state does not change with the cw illumination duration.[20] These conditions are valid for the initial ∼5 s following initiation of cw illumination for isolated RCs because slow light-induced structural changes occur on a time scale longer than the period of a single RC turnover. Therefore, bleaching amplitudes measured for isolated RCs at 5 s are suitable starting points for saturation absorption curves. Because, in these experiments, ∼40% of the isolated RCs contain an active ubiquinone in the Q_B site, they may be considered as two independent systems with each of the two systems approximated as a two-level scheme of electronic transitions.[20] Consequently, the Langmuir expression for these isolated RCs may be written as follows

$$T_{max}(I') = 0.4\frac{\beta I'}{\beta I' + (10\tau_{AP})^{-1}} + 0.6\frac{\beta I'}{\beta I' + (\tau_{AP})^{-1}} \quad (5a)$$

in which the first term on the right-hand side describes the Langmuir dependence for the portion of RCs containing a ubiquinone molecule in the Q_B site and the second term corresponds to RCs with only the Q_A site occupied with a ubiquinone. $I' = I_{ex}/I_0$ is the normalized photoexcitation intensity, $\beta I'$ is the number of RC photoactivation events per unit time, and β is the coefficient that relates the experimentally measured photoexcitation intensity to the corresponding theoretical quantity in s⁻¹. τ_{AP} in eq 5a gives the average survival time of the charge-separated state for RCs lacking a ubiquinone molecule in the Q_B site. Note that the corresponding value for RCs containing an active ubiquinone in the Q_B site is well known to be approximately 10 times larger than τ_{AP}, and this is taken into account by the multiplier 10 in the first term of the right-hand side of eq 5a.[22,23]

Membrane-bound RCs may be considered as a single-component system, in which all the macromolecules actively participate in the $Q_A{}^-$ to Q_B electron transfer. The average survival time of the charge-separated state for the membrane-bound RCs is 3−5 times longer than it is for Q_B containing isolated RCs; see Figure 8a below and the corresponding discussion. This means that bleaching amplitude readings taken at 15 s following the initiation of cw illumination are suitable starting points for saturation absorption curves for membrane-bound RCs. Thus, the Langmuir expression for membrane-bound RCs may be written as follows

$$T_{max}(I') = \frac{\beta I'}{\beta I' + (50\tau_{AP})^{-1}} \quad (5b)$$

in which the term $50\tau_{AP}$ describes the average survival time of the charge separated state.

In Figure 5, the bleaching amplitudes T_{max} from Figures 1 and 2 at 5 s for isolated RCs and at 15 s for membrane-bound RCs are plotted vs normalized actinic light intensity $I' = I_{ex}/I_0$ for the membranes with myxothiazol (■), membranes with myxothiazol and antimycin (○), and isolated RCs (△). Solid lines represent best-fit results of experimental dependencies for the saturation absorption curves given by eqs 5a and 5b. The best-fit values for the coefficient β, the lifetime τ_{AP}, and the χ^2 values for each sample are summarized in Table 1.

The coefficient β is >10 times larger for membrane-bound RCs than for isolated RCs. Thus the relative excitation efficiency
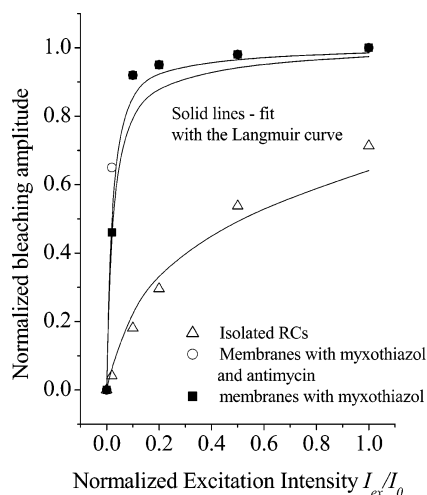
Figure 5. Bleaching amplitude vs normalized photoexcitation intensity for isolated RCs (△), membrane-bound RCs with added myxothiazol (■), and membrane-bound RCs with added myxothiazol and antimycin (○). Solid lines show the best-fit results of modeling with a Langmuir-type dependence. See eqs 5a and 5b in the text.

TABLE 1: Best-Fit Results for Isolated RCs and Membrane-Bound RCs

sample	χ^2	β, s^{-1}	τ_{AP}, s
membranes with myxothiazol	0.00938	138	0.14
membranes with myxothiazol and antimycin	0.00083	183	0.18
isolated RCs	0.00310	9.4	0.09

for membranes is at least 10 times larger than that for isolated RCs at the same incident actinic light intensity I_{ex}. This result suggests that multiple photon-scattering may occur in samples of membrane-bound RCs, causing a greater quantum efficiency of excitation and facilitating enhanced saturation of optical absorption in these samples. This effect is always observed for membrane-bound RCs, but the magnitude of the effect depends on the membrane concentration. In particular, a small difference in β values for the two different samples with membrane-bound RCs in Table 1 should be attributed to the effect of different concentration of the two samples.

Effects of Multiple Actinic Light Flashes Applied to Preilluminated Samples. As we have recently shown, structural memory effects induced by adaptation to a charge-separated state in isolated RCs may be probed in experiments using a sequence of actinic flashes applied to a preilluminated sample.[1,2] The results of similar experiments on membrane-bound RCs are presented in this section.

Figure 6a shows the transient transmittance of a sample of membrane-bound RCs with myxothiazol in a 1-cm path length cuvette. The transmittance was measured upon illumination of the sample for 300 s (optical flux density $P_{cw} \approx 4.5$ mW/cm², excitation wavelengths $\lambda_{cw} = 600-900$ nm) followed by a sequence of short saturating laser flashes spaced at 100-s time intervals (flash energy density $P_{flash} \leq 50$ mJ/cm², $\lambda_{flash} = 605$ nm). Figure 6c shows the result of a similar experiment made with isolated RCs (in a 0.05% LDAO solution) and described previously in ref 2. The light sources and their intensities were the same in both experiments. The illumination protocol in the experiment with isolated RCs was slightly different; a 200-s duration cw illumination was followed by actinic flashes with a 250-s spacing time. In each experiment, the first flash in a train was triggered 5 s after cessation of the cw illumination. Reference curves without laser flashes are shown in each figure. The slow relaxation phase with a time constant $\gg 10$ s, which
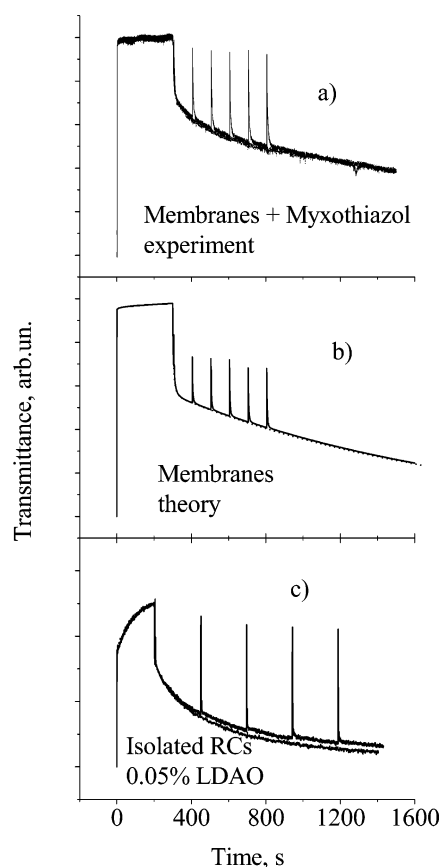

Figure 6. Membrane-bound RC (graph a) and isolated RC (graph c) transmittance changes (at 865 nm) following a stepwise variation of actinic light intensity. The cw actinic light ($I \approx 4.5$ mW/cm², $\lambda_{exc} = 600-900$ nm) was initiated at $t = 5$ s and was stopped at $t = 305$ s (graph a) or $t = 205$ s (graph c). A train of actinic flashes was applied 5 s after turning off the cw actinic light. Transmittance changes following the first flash are not resolved on the graphs. The reference signals measured in separate runs without actinic flashes are also shown on the graphs. Graph b presents the results of numeric modeling for membrane-bound RCs. See text for more details.

was not observed in a single flash activated kinetics applied to a dark-adapted sample (see, e.g., Figure 8a below), was observed after each pulse in a sequence. The accumulation of this phase was slightly lower in the case of the membrane-bound RCs than for isolated RCs with LDAO. See graphs a and c in Figure 7. The amplitude of the very slow equilibration phase following each flash in the train characterizes the amplitude and the time constant of the slow structural relaxation in the charge neutral state of preilluminated samples.[1,2] The time constant for electronic equilibration $\tau_{el} = (I + k_{AP} e^{-x})^{-1}$ is quite long for the light-adapted conformational state of RCs, for which $x = x_B \geq 7.5$. The probability for this state to be probed by a sequence of pulses depends on the population of the charge neutral state with an x value close to x_P prior to each pulse in a sequence. The charge-neutral state population is a function of both the electronic equilibration time at $x \approx x_B$, $\tau_{el}^B = (I + k_{AP} e^{-x_B})^{-1}$ and the structural diffusion constant D_P in this state. Therefore, the results of the above experiments indicate that the structural relaxation (diffusion) in the charge-neutral state of membrane-bound RCs is faster than it is for isolated RCs. Results for the membrane-bound RCs with both myxothiazol and antimycin were very similar to those described above for the membranes with myxothiazol only (not shown in the figures).
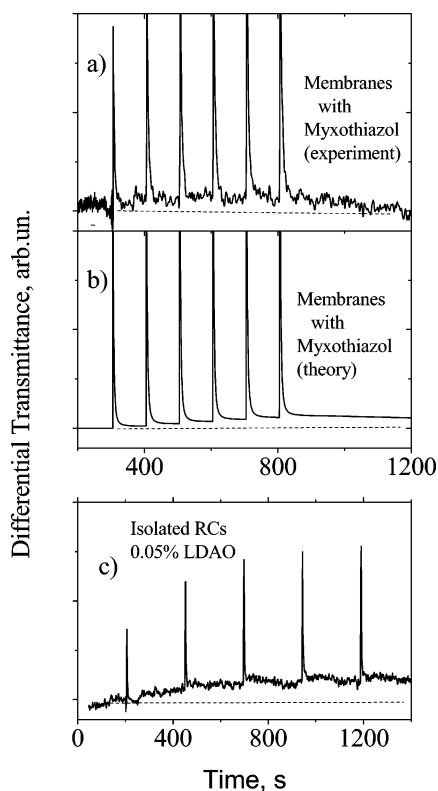
Nonequilibrium Dynamics in Reaction Centers

J. Phys. Chem. B, Vol. 108, No. 8, 2004 **2723**

Figure 7. The difference between traces recorded with applied actinic flashes and reference traces for the membrane-bound RCs (graph a) and isolated RCs (graph c). Graph b presents a corresponding difference trace for the model described in Figure 6b and in the text.

Figure 6b shows the modeling results for membrane-bound RCs using eqs 1−4. The calculation details are described in ref 1. In these modeling studies, when cw actinic light of equal intensity was used for both isolated and membrane-bound RCs, the effective photoexcitation intensity used in the theoretical calculations was 10 times higher for the membrane-bound RCs than the corresponding parameter for isolated RCs. This agrees with our experimental findings that the effective photoexcitation intensity increases greatly for membrane-bound RCs due to multiple scattering effects. The difference between the result calculated for the case with laser pulses "on" and the reference run with the pulses "off" is shown in Figure 7b. Note a close similarity of experimental and theoretical results for the membrane-bound RCs (graphs a and b in Figure 7, respectively) as well as their similarity to the results for isolated RCs with LDAO (graph c in Figure 7).

The accumulation of a slow relaxation component following one flash in a sequence of actinic flashes has not been observed experimentally without cw preillumination of the membranes. See Figure 8, in which graph a shows a single flash activated transient kinetics of the membrane-bound RCs and graph b shows a sequence of seven actinic flashes spaced at 100-s time intervals with no cw preillumination applied.

Discussion

The experimental results on light-induced bleaching kinetics and absorption recovery kinetics in membrane-bound RCs presented in this work show that the dynamic behavior of RCs embedded in membranes is very similar to that of the isolated RCs. Both the isolated and membrane-bound RCs show a pronounced, slow equilibration phase following turning on and off of cw actinic light. Recent studies on isolated RCs proved that the slow kinetic phase is related to the formation and decay
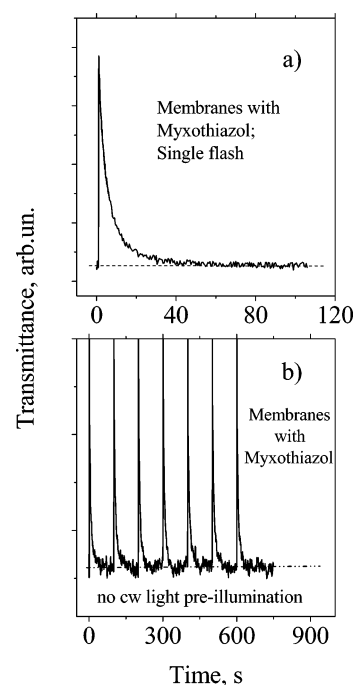

Figure 8. Flash-activated absorption recovery kinetics of dark-adapted membrane-bound RCs with myxothiazol (graph a). Graph b shows the response of the same sample to a train of saturating actinic flashes spaced at 100-s time intervals. No cw preillumination was applied. Note the absence of a buildup of the very slow charge recombination phase following the flashes in the sequence.

of the long-lived charge-separated state $P^+(Q_AQ_B)^-$.[24] This state was presumed to be formed as a result of accumulated structural changes induced by multiple, light-activated consecutive turnovers of RCs. It was shown to originate from nonequilibrium dynamic transitions of the charge-conformational system of RCs.[1−3,19,20] The present studies show that the same dynamic behavior is characteristic of membrane-bound RCs. In particular, our studies show that the system reaction to a saturating, cw actinic light and a train of short actinic flashes is nearly the same for membranes without additional cytochrome bc1 inhibitors and for the membranes with different combinations of inhibitors added. Moreover, this reaction of membrane-bound RCs mimics the behavior of isolated RCs with addition of the detergent LDAO under the similar experimental conditions. See, e.g., Figures 6 and 7.

Results of modeling of photoexcitation bleaching and absorbance recovery kinetics of membrane-bound RCs show that the system behavior can be well described theoretically using almost the same set of parameters as are used to model isolated RCs. There are three important differences however. One is that the effective photoexcitation intensity I_{eff} is at least 10 times higher for the membrane case than for the case of isolated RCs at the same cw actinic light intensity I_{ex}. Another difference is that the structural diffusion constant D_P for membrane samples is several times larger than for isolated RCs with 0.05% LDAO. Finally, the conformational coordinate in the dark adapted state x_P has a value for membranes that is larger by at least 1.5 units than the corresponding value for isolated RCs. See Table 2 for the comparison of modeling results for membrane-bound and isolated RCs.

The slow, generalized structural variable x in our model is defined as $x = \Delta G_{AB}/k_BT$, see eq 1. Therefore, the conformational coordinate value in the dark-adapted state, x_P, is defined via the Gibbs free energy difference for the electron localized either on Q_A or Q_B, $x_P = \Delta G^0_{AB}/k_BT$. The difference of 1.5

TABLE 2: Parameters of the Model for the Membrane-Bound and Isolated RCs

sample	I_{eff}	$x_P{}^a$	x_B	k_P	k_B	α_P	α_B	γ_P	γ_B	k_{AP}	D_P	D_B
RCs in membranes	10	3.5	9	10	10	0.3	0.04	0.9	1.4	10	2.0	0.03
isolated RCs with LDAO^b	1	2	8	10	10	0.07	0.07	1.1	1.1	10	0.5	0.05

^{a} The value $x_P = \Delta G_{AB}/k_BT = 2$ was taken from the literature,[20] as well as $k_{AP} = 10$ for isolated RCs.[34] ^{b} Data were taken from ref 2.

units between the x_P value for chromatophores and isolated RCs corresponds to ~38 meV difference in ΔG_{AB}^0 at room temperature (note that $k_BT_{room} \approx 25$ meV). This result is in a good agreement with a large number of studies of the thermodynamics and kinetics of *Rb. sphaeroides* chromatophores that yielded a value of ~85–120 meV for ΔG_{AB}^0.[25-30] The value of ΔG_{AB}^0 is ~60 meV for isolated *Rb. sphaeroides* RCs.[22,31]

The charge recombination pathway for an electron localized on Q_B in membrane-bound RCs should be the same as for isolated RCs under the normal physiological conditions. The charge recombination occurs in a indirect way via the primary quinone acceptor Q_A.[22,31] Our analysis of single flash-activated charge recombination kinetics shown in Figure 8a with a single-exponential decay function gives a recombination rate constant of $k_{rec} \approx 0.25$ s^{-1}, a value that is in reasonable agreement with the estimate $k_{rec} \approx k_{AP} \exp(-x_P) \approx 0.3$ s^{-1} using $k_{AP} = 10$ s^{-1} and $x_P = 3.5$. We consider only the indirect pathway for charge recombination $P^+Q_AQ_B^- \rightarrow PQ_AQ_B$ in the present work. Our results show that the adaptation of structure to charge separation during multiple turnover events of a RC results in a lowering of the $P^+Q_AQ_B^-$ energy by several k_BT units. In accord with the Marcus theory, such a lowering of the $P^+Q_AQ_B^-$ energy causes a simultaneous decrease in the rate constant for both the indirect and direct ET pathway at a given reorganization energy.[32] Several studies demonstrated that the ET pathway can be switched from an indirect route to the direct one either in mutant RCs, in which the reorganization energy of $P^+Q_AQ_B^-$ state is modified by a protein environment mutation,[31] or by using a ubiquinone substitution in the Q_A site with a lower potential.[23,33] Neither of these two possibilities applies to the case of a charge-separation induced increase of ΔG_{AB}^0 during multiple, consecutive turnover events of an RC.

The magnitude of the structural diffusion constant in the charge neutral state, D_P, determines the extent of structural memory effects in RCs.[1,2] The value of D_P dictates the particular experimental protocol required to observe the structural memory effects. In particular, if the diffusion constant D_P is small, the accumulation of RCs in a long-lived, charge-separated state $P^+(Q_AQ_B)^-$ proceeds efficiently and imparts a significant amplitude of a very slow relaxation component in transient kinetics for preilluminated RCs following each flash in a pulsed excitation train. Such a situation occurs typically for isolated RCs with either Triton × 100 or Na cholate.[1,2] In contrast, at large D_P, the corresponding transient absorption kinetics in RCs may result in a very small amplitude for a slow relaxation component. This case occurs for isolated RCs with LDAO and membrane-bound RCs. In the latter case, a competition between structural diffusion from the "light-adapted" conformational state to the "dark-adapted" conformational state with the charge recombination process that enriches the population of the "light" conformational state with charge-neutral molecules, favors a rapid depletion of the "light" conformational state of the reaction centers with the deformed structure.[2]

An experimental protocol, in which probing flashes are separated significantly in time from each other, is not optimal for experimental characterization of nonequilibrium dynamic effects that originate from the structural memory effects in macromolecules. The time separation between actinic flashes

in experiments such as those shown in Figure 6 must be greater than the time of a complete charge recombination event following a single saturating actinic flash applied to a dark adapted sample. This requirement was fulfilled in the experiments shown in Figure 6. At the same time, such experimental conditions produce very small amplitude of the slow recombination component following each flash in a train. However, despite a considerably faster structural relaxation time in the charge neutral state of the membrane-bound RCs in comparison with that for the isolated RCs, the efficiency of accumulated structural changes in the "light-adapted" conformational state seems to be higher for the chromatophores because of a drastic increase in the effective excitation intensity I_{eff}.

Conclusion

This work consists of two independent parts, one characterizing, for the first time, multiple scattering effects for chromatophores and the other describing studies of nonequilibrium dynamic properties of RCs embedded in membranes. The results obtained show that in highly disordered systems of photosynthetic membranes the photoactivation probability for each RC is significantly enhanced due to multiple scattering effects; therefore, actinic light of a comparatively low intensity induces a fast saturation of RC absorption, thus facilitating an RC structural transition into the "light-adapted" conformational state. Experiments with a sequence of saturating actinic flashes applied to a preilluminated sample indicate that structural memory effects, though not as pronounced as in the isolated RCs, do occur and play an important role in the function of membrane-bound RCs.

References and Notes

(1) Barabash, Yu. M.; Berezetskaya, N. M.; Christophorov, L. N.; Goushcha, A. O.; Kharkyanen, V. N. *J. Chem. Phys.* **2002**, *116*, 4339–4352.

(2) Goushcha, A. O.; Manzo, A. J.; Scott, G. W.; Christophorov, L. N.; Knox, P. P.; Barabash, Yu. M.; Kapoustina, M. T.; Berezetska, N. M.; Kharkyanen, V. N. *Biophys. J.* **2002**, *84*, 1146–1160.

(3) Barabash, Y. M.; Zabolotnyi, M. A.; Sokolov, N. I.; Kharkyanen, V. N. *Biophysics* **2002**, *47*, 896–902.

(4) Crofts, A. R.; Wang, Z. G. *Photosynthesis Research* **1989**, *22*, 69–87.

(5) Okeefe, D. P.; Prince, R. C.; Dutton, P. L. *Biochim. Biophys. Acta* **1981**, *637*, 512–522.

(6) Gray, K. A.; Daldal, F. In *Anoxygenic Photosynthetic bacteria*; Blankenship, R. E., Madigan, M. T., Bauer, C. E., Eds.; Kluwer: The Netherlands, 1995; pp 747–774.

(7) Meinhardt, S. W.; Crofts, A. R. *FEBS Lett.* **1982**, *149*, 223–227.

(8) Jones M. R.; Visschers, R. W.; van Grondelle, R.; Hunter, C. N. *Biochemistry* **1992**, *31*, 4458–4465.

Nonequilibrium Dynamics in Reaction Centers

J. Phys. Chem. B, Vol. 108, No. 8, 2004 **2725**

(9) Berry, E. A.; Guergova-Kuras, M.; Huang, L. S.; Crofts, A. R. *Annu. Rev. Biochem.* **2000***, 69*, 1005−1075.

(10) Von Jagow, G.; Link, T. A. *FEBS Lett*. **1986**, *237*, 31−34.

(11) Von Jagow, G.; Engel, W. D. *FEBS Lett*. **1981**, *136*, 19−24.

(12) Dogariu, A.; Boreman, G. D.; Dogariu, M. *Optics Lett*. **1995**, *20*, 1665−1667.

(13) Zhang, W.; Cue, N.; Yoo, K. M. *Optics Lett*. **1995**, *20*, 1023−1025.

(14) Sajeev, J.; Pang, G. *Phys. Rev. A*. **1996**, *54*, 3642−3652.

(15) Rivas, J. G.; Sprik, R.; Soukoulis, C. M.; Busch, K.; Lagendijk, A. *Europhys. Lett.* **1999**, *48*, 22−28.

(16) Straley, S. C.; Parson, W. W.; Mauzerall, D. C.; Clayton, R. K. *Biochim. Biophys. Acta* **1973**, *305*, 597−609.

(17) Feher, G.; Okamura, M. Y. In *The Photosynthetic Bacteria*; Clayton, R. K., Sistrom, W. R., Eds.; Plenum Press: New York, 1978; pp 349−386.

(18) Lin, S.; Katilius, E.; Haffa, A. L. M.; Taguchi, A. K. W.; Woodbury, N. W. *Biochemistry* **2001**, *40*, 13767−13773.

(19) Abgaryan, G. A.; Christophorov, L. N.; Goushcha, A. O.; Holzwarth, A. R.; Kharkyanen, V. N.; Knox, P. P.; Lukashev, E. A. *J. Biol. Phys.* **1998**, *24*, 1−17.

(20) Goushcha, A. O.; Kharkyanen, V. N.; Scott, G. W.; Holzwarth, A. R. *Biophys. J.* **2000**, *79*, 1237−1252.

(21) Knox, P. P.; Lukashev, E. P.; Timofeev, K. N.; Seifullina, N. K. *Biochemistry* **2002**, *67*, 901−907.

(22) Kleinfeld, D.; Okamura, M. Y.; Feher, G. *Biochim. Biophys. Acta* **1984**, *766*, 126−140.

(23) Labahn, A.; Bruce, J. M.; Okamura, M. Y.; Feher, G. *Chem. Physics* **1995**, *197*, 355−366.

(24) Van Mourik, F.; Reus, M.; Holzwarth, A. R. *Biochim. Biophys. Acta* **2001**, *1504*, 311−318.

(25) Arata, H.; Nishimura, M. *Biochim. Biophys. Acta* **1983**, *725*, 394−401.

(26) Arata, H. *Biochim. Biophys. Acta* **1985**, *809*, 284−287.

(27) Rutherford, A. W.; Evans, M. C. W. *FEBS Lett*. **1980**, *110*, 257−261.

(28) Cherepanov, D. A.; Bibikov, S. I.; Bibikova, M. V.; Bloch, D. A.; Drachev, L. A.; Gopta, O. A.; Oesterhelt, D.; Semenov, A. Y.; Mulkidjanian, A. Y. *Biochim. Biophys. Acta−Bioenerg.* **2000**, *1459*, 10−34.

(29) Ginet, N.; Lavergne, J. *Biochemistry* **2000**, *39*, 16252−16262.

(30) Tandori, J.; Nagy, L.; Puskas, A.; Droppa, M.; Horvath, G.; Maroti, P. *Photosynth. Res.* **1995**, *45*, 135−146.

(31) Labahn, A.; Paddock, M. L.; McPherson, P. H.; Okamura, M. Y.; Feher, G. *J. Phys. Chem.* **1994**, *98*, 3417−3423.

(32) Marcus, R. A.; Sutin, N. *Biochim. Biophys. Acta* **1985**, *811*, 265−322.

(33) Li, J.; Takahashi, E.; Gunner, M. R. *Biochemistry* **2000**, *39*, 7445−7454.

(34) Kleinfeld, D.; Okamura, M. Y.; Feher, G. *Biochemistry* **1984**, *23*, 5780−5786.